Friction **11**(7): 1177–1193 (2023)
https://doi.org/10.1007/s40544-022-0645-2
ISSN 2223-7690
CN 10-1237/TH
RESEARCH ARTICLE

Cartilage-bone inspired the construction of soft-hard composite material with excellent interfacial binding performance and low friction for artificial joints

Qin CHEN[1,3,†], Xinyue ZHANG[2,†], Siyu LIU[1], Kai CHEN[1,4,5,*], Cunao FENG[1], Xiaowei LI[1], Jianwei QI[1], Yong LUO[1], Hongtao LIU[1], Dekun ZHANG[1,*]

[1] *School of Materials Science and Physics, China University of Mining and Technology, Xuzhou 221116, China*

[2] *School of Mechatronic Engineering, China University of Mining and Technology, Xuzhou 221116, China*

[3] *School of Chemical Engineering and Technology, China University of Mining and Technology, Xuzhou 221116, China*

[4] *State Key Laboratory of Solid Lubrication, Lanzhou Institute of Chemical Physics, Chinese Academy of Sciences, Lanzhou 730000, China*

[5] *State Key Laboratory of Tribology, Tsinghua University, Beijing 100084, China*

Received: 22 October 2021 / Revised: 25 January 2022 / Accepted: 04 May 2022

Abstract: Inspired by the cartilage-bone structure in natural joints, soft-hard integrated materials have received extensive attention, which are the most promising candidates for artificial joints due to their combination of excellent load-bearing properties and lubricating properties. The latest progress showed that the combination of hydrogel and titanium alloy can realize a bionic natural joint lubrication system on the surface of titanium alloy. However, obtaining a tough interface between the hydrogel (soft and wet) and the titanium substrate (hard and dry) is still a great challenge. Here, we designed a "soft (hydrogel)-hard (Ti6Al4V)" integrated material with outstanding combination, which simulates the structure and function of cartilage-bone in the natural joint. The load-bearing properties, binding performance, and tribological behaviors for different forms of the soft-hard integrated materials were investigated. The results showed that the hydrogel layer and Ti6Al4V substrate possess ultra-high interfacial toughness (3,900 J/m^2). In addition, the combination of the hydrogel layer and Ti6Al4V substrate provided a good lubrication system to endow the "soft (hydrogel)-hard (Ti6Al4V)" integrated material with high load-bearing and excellent tribological properties. Therefore, this study provided an effective strategy for prolonging the service life of Ti6Al4V in the biomedical field.

Keywords: Ti6Al4V alloy; hydrogel; soft-hard interface; friction

1 Introduction

Articular cartilage is a soft tissue with significant functions covering the ends of the joint bones. It provides an excellent lubricating and bearing joint surface, which can transmit 7–9 times the weight of the human body and maintain an extremely low friction coefficient (0.001–0.04) [1, 2]. Cartilage would be injured due to various factors such as the increase in age, congenital diseases, abrasion, or trauma. However, articular cartilage is difficult to repair itself after damage due to its avascular and limited self-healing capacity, which may lead to the occurrence of osteoarthritis and seriously affect the quality of life of patients [3, 4]. Therefore, it is necessary to explore effective methods to repair or replace the damaged articular cartilage, and then reconstruct the function of the joint.

Currently, joint replacement was considered an effective method for treating osteoarthritis. The

† Qin CHEN and Xinyue ZHANG contributed equally to this work.

* Corresponding authors: Kai CHEN, E-mail: cumtck@cumt.edu.cn; Dekun ZHANG, E-mail: dkzhang@cumt.edu.cn

commonly used artificial joint materials are mainly metal materials, ceramic materials, and ultra-high molecular weight polyethylene [5–7]. Among them, titanium alloy has been widespread concerned in artificial joint materials because of its excellent mechanical performances, high biocompatibility, fatigue resistance, and corrosion resistance [8, 9]. Therefore, titanium can form long-term and effective interaction with soft tissues and bone to replace damaged joints [10–12]. Although titanium and its alloys have been used clinically in the middle of the last century, there are still some shortcomings in their surface characteristics, which affect their service life in many applications. For instance, titanium alloys as artificial joints can produce wear debris, release metal ions, and cause bone dissolution around the prosthesis, resulting in the failure of joint materials after long-term friction [13]. The existence of articular cartilage can keep the joints with excellent boundary lubrication under high load and lower speed bending. Thus, a bionic lubricating cartilage layer should be designed on the surface of hard artificial joint materials by surface modification technology to make it similar to natural human joints in structure and function, which is the most attractive method to enhance the bio-tribology of titanium alloy surfaces. For example, hydrophilic polymer coatings have been developed for surface modification of titanium and its alloys [14–16].

Hydrogels were considered to be the most promising substitute for artificial articular cartilage by their good biocompatibility, adjustable mechanical properties, excellent biotribological properties, and the similarity of the microstructure of natural cartilage [17, 18]. Recently, inspired by the structure and functions of the cartilage, hydrogels have received widespread attention as a coating for hard artificial joint materials, which can dramatically moderate the friction effect of hard materials due to soft and moist characteristics [19, 20]. Among them, polyvinyl alcohol (PVA) hydrogels have received extensive attention as a substitute for articular cartilage because of their excellent biocompatibility, and biotribological properties [17, 21, 22]. However, the traditional PVA hydrogels are weak and brittle, which is difficult to meet the requirements of articular cartilage. Therefore, various methods (double or triple network structure, nano/micro materials reinforcement, annealing, etc.) have been developed to enhance the mechanical properties of the hydrogels [17, 23, 24]. Despite the excellent mechanical properties, outstanding lubricating performance, and biological activity are also the criteria for hydrogels as the cartilage substitute. Therefore, we should be chosen biocompatible materials as additives to promote the mechanical properties, bioactivity, and biotribological properties of PVA hydrogel. As far as we know, nano-hydroxyapatite (HA) is the main inorganic phase of bones, which can achieve chemical bonding with tissues, then stimulate or induce bone hyperplasia, and promote the repair of defective tissues. It showed that nano-hydroxyapatite (HA) with excellent biocompatibility and biological activity [25, 26]. Moreover, HA as an inorganic nanofiller in the hydrogel plays a role in the enhancement of mechanical properties (nanoparticle reinforcement) and tribological properties (HA can interact with polymer chains to enhance the network structure, which can decrease the deformation and contact area of the hydrogel during the friction tests). The studies showed that the load-bearing capacity, biological activity, and tribological performance of hydrogels were improved by the addition of HA [17, 27, 28]. Polyacrylic acid (PAA) is a hydrophilic polymer with a largr number of carboxyl groups, which can hydrogen bonding with other polymer chains to form the interpenetrating network, showing higher mechanical properties [7, 17]. Also, studies have shown that PAA can improve the surface roughness and biocompatibility of the hydrogel [29]. At present, PAA has been widely used in tissue engineering [30, 31]. In summary, our hydrogel layer takes PVA, HA, and PAA as the main materials.

In addition, a substantial obstacle to coating a soft, wet hydrogel on a hard substrate is how to obtain a strong bonding between them. Most of the methods connecting hydrogel with the substrate are through physical bonding, which cannot achieve strong bonding at the interface. Recent reports illustrated that mechanical interlocking and chemical bonding have been used to obtain a tough soft-hard interface [32–35]. Kurokawa et al. [35] utilized the double-network principle to anchor the dual-network (DN) hydrogel in a porous solid substrate, which built a strong interface between a DN gel and a porous solid. To

obtain both high mechanical properties and excellent tribological performance of materials for artificial joints, Zhou et al. [20] used laser processing and surface sulfonation to prepare porous laser and sulfonation poly(ether-ether-ketone) (LSPEEK), and then cast PVA hydrogel on the surface of LSPEEK to simulate natural cartilage-subchondral bone in structure and function successfully. Yuk et al. [36] realized the covalent immobilization of the long-chain polymer network of a hard hydrogel on a non-porous solid surface through silanization of the substrate surface. The above studies have improved the binding force between the hydrogel and the hard substrate to a certain extent, but it is still a challenge to meet both the high mechanical properties of the hydrogel and the tough interface for long-term stability. Based on mussels can adhere to almost all inorganic and organic surfaces and maintain strong adhesion even in humid environments, polydopamine (PDA) was widely used to increase the adhesion of materials due to the presence of catechol [19, 34, 37], we hypothesized that the introduction of PDA coating on titanium alloy surface can effectively improve the binding performance of the soft-hard interface by chemical adhesion. Moreover, PDA has attracted more and more attention as an additive in hydrogels that can promote cell adhesion and provide the excellent biocompatibility to hydrogels [38–40]. Therefore, the introduction of PDA can not only enhance the binding performance but also improve the biocompatibility of the soft-hard integrated material.

Here, inspired by the structure of natural joints and the multifunctional adhesion characteristics of mussels, we proposed a "soft surface-hard substrate" approach to design soft-hard integrated materials for artificial joints, which can obtain both high mechanical properties and excellent tribological properties. We initially processed the Ti6Al4V alloy by laser processing and PDA surface modification. Then, PVA/HA/PAA/PDA hydrogel was cast on the Ti6Al4V by freezing-thawing technology, achieving a tough soft-hard integrated material. Mechanical interlocking was formed between the hydrogel and the Ti6Al4V substrate, and the PDA on the Ti6Al4V substrate can interact with hydrogel by chemical adhesion, effectively enhancing the binding between the hydrogel and the substrate. In addition, the tribological properties of soft-hard materials were rarely studied. However, the tribological properties are of great significance to the use of hydrogel-Ti6Al4V integrated materials as artificial joint implants. In this work, the sliding, twisting, and swinging tribological behaviors of the hydrogel-Ti6Al4V integrated material are studied by simulating the motion form of the human body, and the results showed that the material has excellent tribological properties.

2 Experimental

2.1 Materials

PVA (Polymerization degree: 1,750 ± 50, alcoholysis degree: more than 99%), ammonium hydroxide ($NH_3{\cdot}H_2O$), and hydrogen peroxide (H_2O_2, 30%) were obtained from Sinopharm Chemical Reagent Co., Ltd. Polyacrylic acid of liquid (PAA, 25 wt%) was purchased from Beijing Yinuokai Technology Co., Ltd. Dopamine hydrochloride (DA) and copper sulfate pentahydrate ($CuSO_4{\cdot}5H_2O$) were purchased by the Shanghai McLean Biochemical Technology Co., Ltd. Nano-Hydroxyapatite (n-HA, 20 nm) was obtained from Nanjing Emperor Nano Material Co., Ltd.

2.2 Pretreatment of titanium alloy (Ti6Al4V)

All Ti6Al4V samples were polished with sandpaper, and then laser treatment was performed on the polished Ti6Al4V surface to obtain porous LTi6Al4V. The samples were ultrasonically cleaned with deionized water and absolute ethanol 3 times to remove wear debris and then dried at 50 °C for 24 h. Next, PDA was used as a coating to modify the surface of the LTi6Al4V. 0.528 g $CuSO_4{\cdot}5H_2O$, and 1.5 g DA were dissolved in 60 mL deionized water to form solution A. Solution B is a mixture of 240 mL deionized water, 120 mL ethanol, 3 mL $NH_3{\cdot}H_2O$, and 0.93 g 30% H_2O_2 solution. Solution B was poured into solution A and stirred evenly to obtain $CuSO_4/H_2O_2$ treatment solution for soaking the LTi6Al4V to form the PDA coating. Finally, the LTi6Al4V was taken out after 2 h and ultrasonically cleaned with ethanol for 15 min to remove excess polydopamine, obtaining a PDA-modified LTi6Al4V substrate (PDA-LTi6Al4V).

2.3 Preparation of Ti6Al4V-hydrogel soft-hard integrated material

The preparation of PDA was prepared according to the previous report [41]. First, 1 wt% PDA was uniformly dispersed in the deionized water by ultrasound for 5 min. Next, 16 wt% PVA, 2 wt% HA, and 4 wt% PAA were added to the PDA solution and stirred at 95 °C for 4–5 h in a water bath to form PVA/HA/PAA/PDA sol. Finally, the sol was poured on the PDA-LTi6Al4V substrate, and subjected to freezing-thawing and annealing treatments (–20 °C to freeze for 6 h, room temperature to thaw for 2 h, repeated 9 times; annealing at 120 °C for 1 h) to obtain Ti6Al4V-Hydrogel soft-hard integrated material.

2.4 Component and morphology characterizations

The surface elementary composition of LTi6Al4V, PDA-LTi6Al4V, and Ti6Al4V substrate after tearing off the hydrogel were characterized by the X-ray photoelectron spectroscopy (XPS, ESCALAB 250Xi, USA). The microscopic morphology of Ti6Al4V-hydrogel was detected by scanning electron field emission scanning electron microscope (FESEM), Hitachi SU8220, Japan), and its element distribution was analyzed by energy dispersive spectroscopy (EDS, XflashFQ5060, Germany).

2.5 Mechanical properties measurement

The compression properties of the Ti6Al4V-Hydrogel were tested by WDW-2 microcomputer-controlled electronic universal testing machine. The samples were cubic (25 mm × 25 mm × 5 mm of Ti6Al4V substrate, and the thickness is 1 mm of hydrogel layer), and the compression test was carried out at a rate of 5 mm/min and a strain of 50%. The compressive strength is obtained by dividing maximum force (F) by the cross-sectional area (S), and the compressive modulus was defined as the slope of the stress–strain curve in the 0–10% strain region. The creep performance was determined by the UMT-Ⅱ multifunctional friction and wear tester. The Ti6Al4V-hydrogel sample was fixed in the lower clamp and the upper sample is CoCrMo ball (diameter: 28 mm) to load the Ti6Al4V-hydrogel sample. During the experiment, the creep load was set as: 5, 10, and 20 N, the creep time was 1 h, and the medium is deionized water.

2.6 Binding strength and interfacial toughness

The binding strength between the Ti6Al4V substrate and hydrogel was tested by the adhesion tester (F510-20T, Elcometer, UK). Fix the Ti6Al4V-hydrogel on the fixture, stick the forging die for the tester on the upper hydrogel and the lower Ti6Al4V substrate of Ti6Al4V-hydrogel, and then pull up the forging die in the direction perpendicular to the Ti6Al4V-hydrogel binding surface until the hydrogel was pulled off the Ti6Al4V substrate by adhesion tester.

The interfacial toughness of Ti6Al4V-hydrogel was detected by the standard 90-degree peeling test. The Ti6Al4V-hydrogel materials were prepared with 50 mm in length, and 25 mm in width. In addition, half of the hydrogel layer was bonded to the substrate, while another half was separated from the substrate. The peeling speed of the 90-degree peeling test was 2 mm/min. In the peeling process, the peel force will enter a stable state (plateau force), that is, the force needed to peel off the hydrogel from the substrate. The interfacial toughness Γ was determined by dividing the plateau force F by the width of the hydrogel sheet W.

$$\Gamma = \frac{F_S}{W} \tag{1}$$

2.7 Friction test

The sliding friction was carried on the UMT-Ⅱ multifunctional friction and wear tester. The friction pair was CoGrMo ball (diameter: 28 mm), the sliding

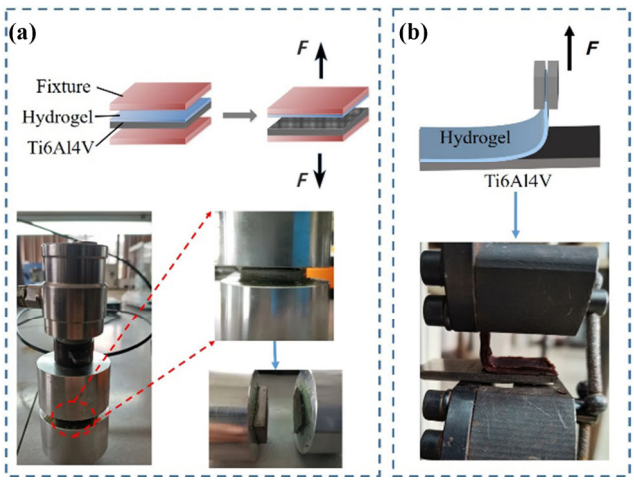

Fig. 1 Schematic diagrams of (a) normal binding test and (b) 90° peel test of the Ti6Al4V-hydrogel integrated material.

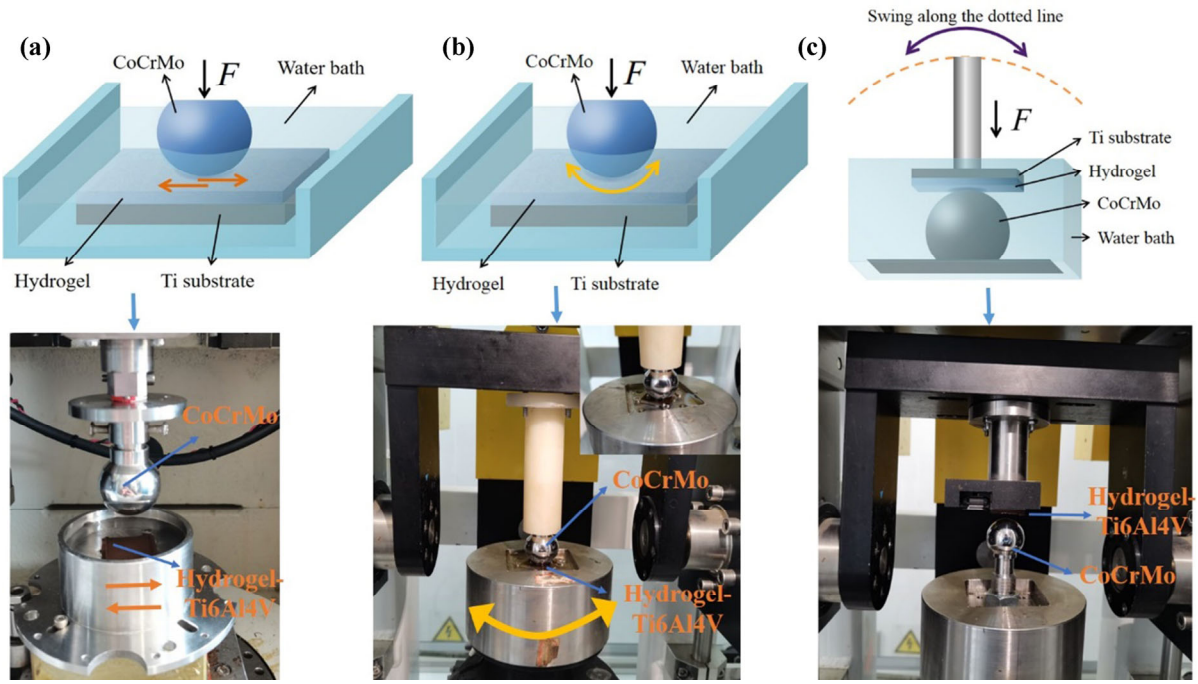

Fig. 2 Schematic diagrams of (a) sliding friction, (b) twisting friction, and (c) swing friction tests.

speeds are 5, 20, and 35 mm/s, the amplitude is 5 mm, the loads are 20, 30, and 40 N, the lubricant is water, and the test time is 30 min.

The Prosim 2 station deep flexion knee simulator was used to determine the twisting friction properties of the Ti6Al4V-hydrogel materials. The friction pair was CoGrMo ball (diameter: 28 mm), the loads are 400, 600, and 800 N, the twisting angle are 5°, 10°, 15°, and 20°, the frequency is 1 Hz, the lubricating medium is deionized water, and the twisting cycle is 2,000.

Similarly, the swing friction of the Ti6Al4V-hydrogel composite was tested by the PROSIM knee joint wear simulator. The friction pair was CoGrMo ball (diameter: 28 mm), the loads are 100, 150, and 200 N, the swing angle are 5°, 10°, 15°, and 20°, the frequency is 1 Hz, the lubricating medium is deionized water, and the swing cycle is 2,000.

2.8 Statistical analysis

In this work, three parallel samples were measured and the final data are reported as means ± SD (standard deviation). Moreover, the calculated results were analyzed by the Tukey test to determine the statistical significance ($p < 0.05$).

3 Results and discussion

3.1 Formation of the Ti6Al4V-hydrogel and basic characterizations

The formation mechanism of Ti6Al4V-hydrogel soft-hard integrated material is shown in Fig. 3. Inspired by the structure and function of articular cartilage-subchondral bone, biomimetic soft-hard integrated material was designed with soft hydrogel and hard Ti6Al4V for artificial joint material. The key point in the formation of Ti6Al4V-hydrogel soft-hard integrated material is the bonding between Ti6Al4V and hydrogel, so it is essential to enhance the bonding between Ti6Al4V and hydrogel by surface modification. The surface modification of Ti6Al4V is mainly composed of two parts. Firstly, the porous structure was formed on the surface of Ti6Al4V by laser printing, and the hydroxylated surface was obtained on the Ti6Al4V substrate at the same time. Secondly, inspired by the adhesion of mussels, PDA was synthesized in situ on the LTi6Al4V surface. PDA can adhere closely to the surface of almost all materials, and the catechol groups in PDA and the –OH on the surface of the Ti6Al4V substrate could be dehydrated to form bidentate coordination bonds, which are firmly attached to

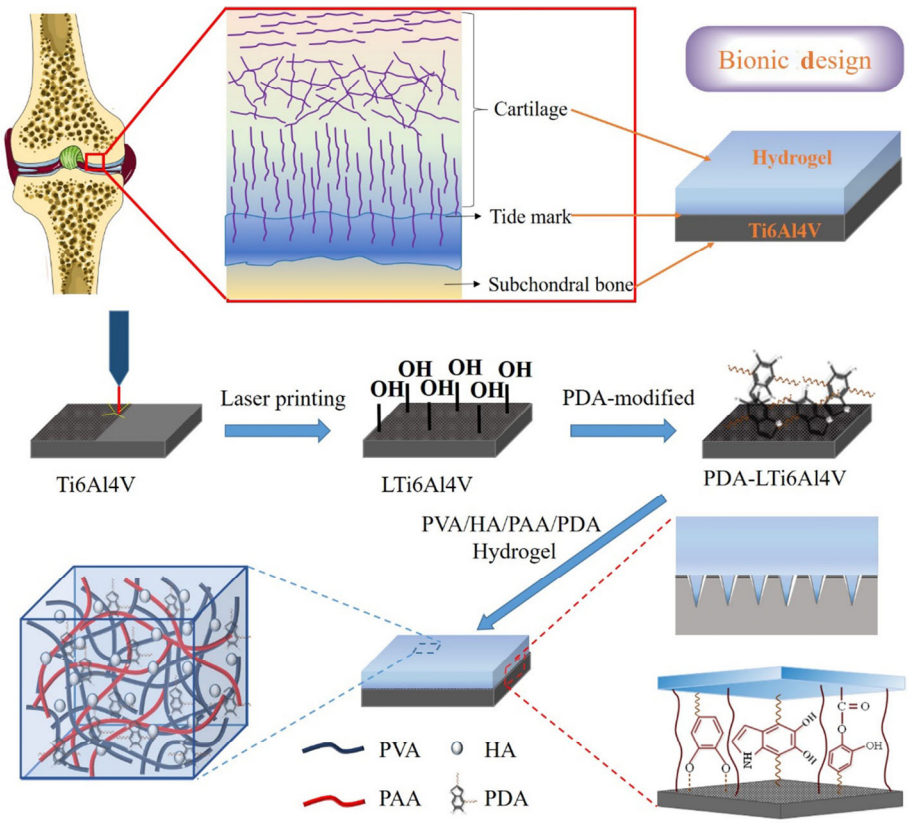

Fig. 3 Schematic illustration of the bionic design of the Ti6Al4V-hydrogel integrated material.

the surface of LTi6Al4V to obtain PDA-LTi6Al4V. In addition, it also can improve the mechanical properties of hydrogels as a nano-reinforcing phase and hydrogen bonding with other polymer chains to enhance the network structure. PVA/HA/PAA/PDA was used as a hydrogel layer to cover the surface of PDA-LTi6Al4V to form the soft-hard integrated structure. PVA/HA/PAA/PDA sol was poured on the PDA-LTi6Al4V surface, and then frozen-thawed to form a gel which was attributed to the formation of the hydrogen bonds and microcrystalline structure. Due to the existence of the microporous structure on the Ti6Al4V substrate surface, the hydrogel can be embedded in the micropores to produce a tight pinning effect with the substrate. Furthermore, the PDA on the Ti6Al4V surface can adhere to the hydrogel due to the multifunctional adhesion, and a large number of hydrogen bonds could be formed between the PDA (Ti6Al4V surface) and the polymer chains so that the hydrogel tightly combined with the Ti6Al4V substrate. Similarly, the PDA in the hydrogel can enhance the adhesion strength of the hydrogel on the Ti6Al4V substrate. Overall, the soft-hard integrated materials Ti6Al4V-hydrogel were successfully prepared by laser fitting, PDA adhesion, and freezing-thawing technology.

In previous work, the basic properties of PVA/HA/PAA/PDA hydrogels were characterized, and the results showed that the porous three-dimensional network structure of PVA/HA/PAA/PDA hydrogels is comparable to the articular cartilage. Moreover, the PVA, PAA, and PDA in the PVA/HA/PAA/PDA hydrogel were well cross-linked [41]. Therefore, the surface of the titanium alloy substrate was characterized by SEM, XPS, and EDS. As shown in Fig. 4(c), a uniformly dense microporous matrix was displayed on the surface of Ti6Al4V substrate by laser printing, which can enlarge the contact area between the hydrogel and the Ti6Al4V substrate. In addition, PDA particles were uniformly and densely distributed on the surface of the substrate, which was conducive to the combination between Ti6Al4V and the hydrogel. Figures 4(a) and 4(b) showed the XPS spectra of the Ti6Al4V substrate to analyze the chemical composition

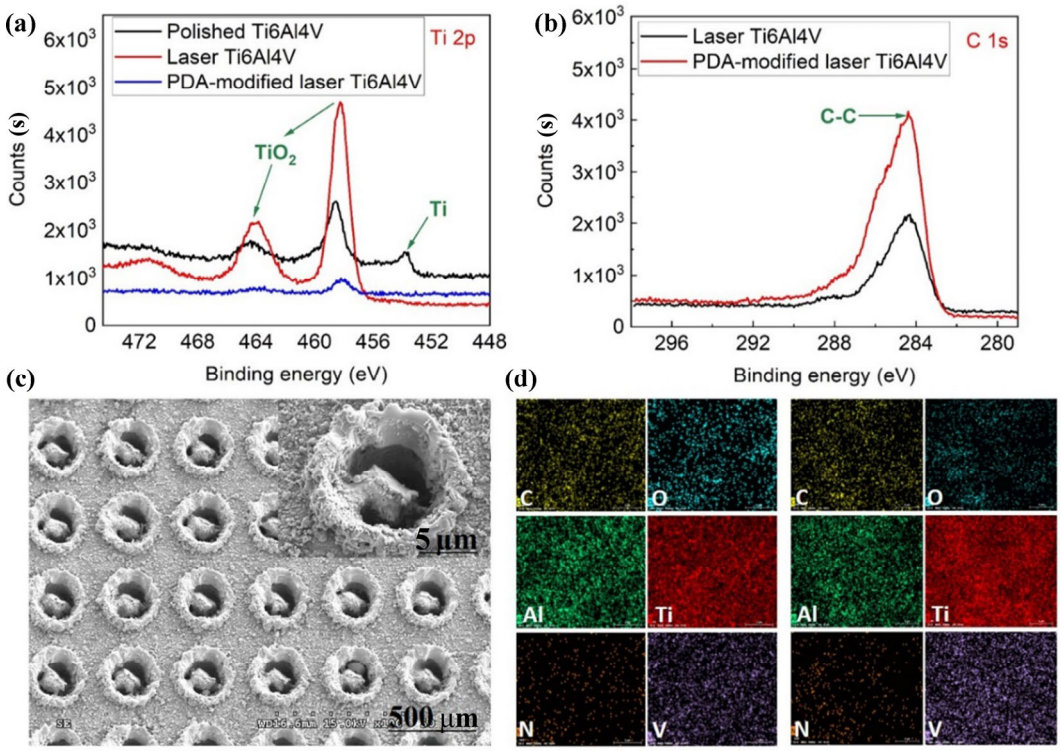

Fig. 4 (a) Ti 2p XPS spectrum of polished Ti6Al4V, L-Ti6Al4V, and PDA-LTi6Al4V; (b) C 1s XPS spectra of polished L-Ti6Al4V and PDA-LTi6Al4V; (c) SEM image of PDA-LTi6Al4V; and (d) EDS diagrams of L-Ti6Al4V and PDA-LTi6Al4V.

in different treatment processes. The Ti 2p narrow scan pattern showed that the characteristic peak of Ti disappeared, while the characteristic peak of TiO_2 increased in LTi6Al4V, indicating that the surface of Ti6Al4V was oxidized to generate TiO_2 (hydroxylated surface). The characteristic peak of TiO_2 significantly weakened, and the characteristic peak of C–C enhanced on the surface of PDA-LTi6Al4V (Fig. 4(b)), which indirectly proved that the PDA modified layer adhered to the surface of Ti6Al4V. Besides, the EDS spectrums indicated that PDA-LTi6Al4V surface has an increase in N content and a decrease in O content compared with LTi6Al4V (Fig. 4(d)). Thus, it is proved that the PDA was attached to the surface of Ti6Al4V.

3.2 Mechanical properties

The mechanical properties of the hydrogel layer are of great significance to the application of soft-hard integrated materials. The results showed that the PDA can significantly enhance the mechanical properties of Ti6Al4V-hydrogel material (Fig. 5). As shown in Fig. 5(a), the typical compression stress-strain curves (50% strain of hydrogel layer) indicated that the hydrogel layer of Ti6Al4V-hydrogel (PVA/HA/PAA/PDA) soft-hard integrated materials has excellent mechanical properties (compressive strength ~2.63 MPa, compressive modulus ~1.56 MPa). Moreover, it is important for artificial cartilage material to endure the successive multiple loading-unloading for a short time. 5 cyclic compression loading-unloading test was performed for the Ti6Al4V-Hydrogel material at a compressive strain of 50% of the hydrogel layer. The hysteresis loops were almost coincided except for the first cycle (Figs. 5(c) and 5(d)). Taking the Ti6Al4V-hydrogel (PVA/HA/PAA/PDA) as an example, the maximum stress of the hydrogel maintained at 2.28 MPa after 5 cyclic compression tests (approximately 86.7% of the first cycle), showing that the hydrogel can recover immediately to withstand repeated loads without being damaged. At the same time, the area of the stress-strain hysteresis loop of the PVA/HA/PAA/PDA hydrogel layer is larger than that of the PVA/HA/PAA hydrogel layer, indicating that the three-dimensional network became denser due to the

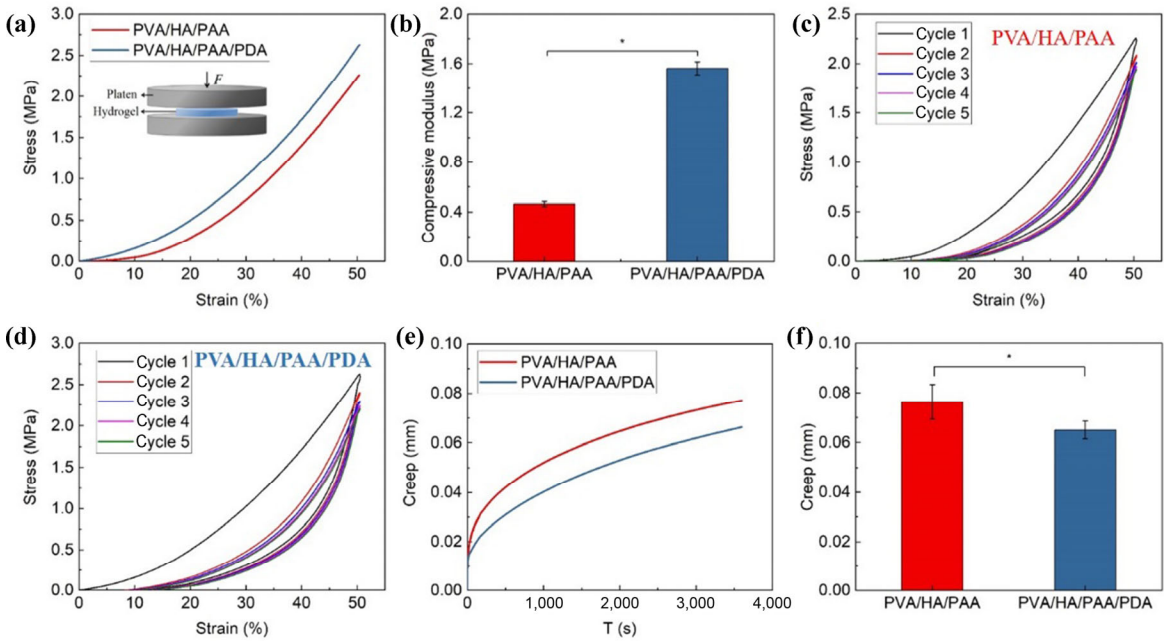

Fig. 5 (a) Typical compressive stress–strain curves and (b) compressive modulus of Ti6Al4V-PVA/HA/PAA hydrogel and Ti6Al4V-PVA/HA/PAA/PDA hydrogel. Stress–strain curve of five continuous compression-relaxation cycles of (c) Ti6Al4V-PVA/HA/PAA hydrogel and (d) Ti6Al4V-PVA/HA/PAA/PDA hydrogel. (e) Creep curves and (f) maximum creep of the Ti6Al4V-PVA/HA/PAA hydrogel and Ti6Al4V-PVA/HA/PAA/PDA hydrogel.

presence of PDA, so that the PVA/HA/PAA/PDA hydrogel layer has better energy dissipation capacity. Similarly, the creep deformation resistance of the Ti6Al4V-hydrogel (PVA/HA/PAA/PDA) materials has been significantly improved, making the hydrogel less deformed under load (Figs. 5(c)–5(f)).

3.3 Evaluation of binding performance between hydrogel layer and Ti6Al4V

The excellent interfacial binding performance is a significant prerequisite to ensure the long-term service life and stability of the artificial joints. We found that the hydrogel was easily separated from the Ti6Al4V when the hydrogel was directly cast on the Ti6AL4V. On the contrary, the hydrogel and the Ti6Al4V exhibited excellent binding performance when the hydrogel was cast on the Ti6Al4V after laser treatment and PDA modification. It can be seen that the excellent combination between the hydrogel and the Ti6Al4V owing to the formation of the mechanical interlocking by the gel embedded into the microporous structure on the Ti6Al4V surface (Figs. 6(a) and 6(b)). The effect of PDA was measured by the binding strength and interfacial toughness.

The uniformly dense microporous matrix was distributed on the surface of the substrate that the hydrogel flowed into the laser micropores to form a mechanical interlocking effect, which can effectively enhance the binding strength between the substrate and the hydrogel [20]. Therefore, we have performed different times of laser processing on the Ti6Al4V substrate. As shown in Fig. 6(c), the interface binding strength of the soft-hard integrated material increased with the increase of the laser treatment times, but the increment of the binding strength of thrice laser treatment is small by comparing to twice laser treatment (there is no significant difference), twice laser treatment was finally selected as the optimal parameters. Similarly, the effect of PDA modification on the binding performance was evaluated by the determination of the binding strength. Figure 6(d) showed that the interface binding strength with or without PDA modification are ~ 52.7 MPa and ~ 41.2 MPa, respectively. Thus it can be seen that the chemical adhesion of the catechol element in the PDA greatly improved the binding strength.

In addition, the interfacial toughness between the substrate and the hydrogel was measured by a

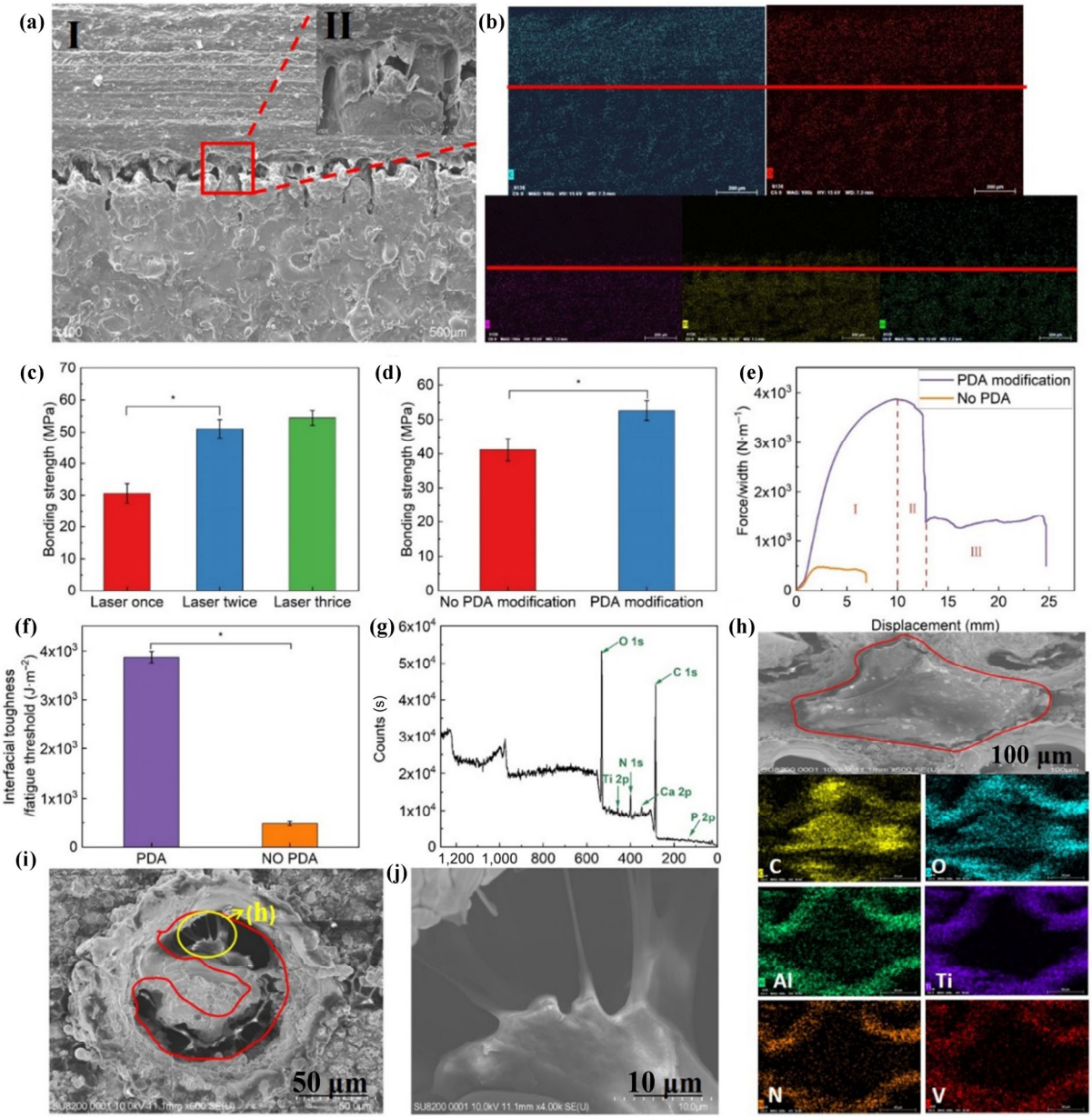

Fig. 6 (a) SEM images and (b) EDS spectrums (C, O, V, Ti, and Al) of the cross-sectional of the soft-hard integrated material. (c) Binding strength between Ti6Al4V substrate and PVA/HA/PAA/PDA hydrogel after once, twice, and thrice laser treatment of Ti6Al4V substrate. (d) Binding strength between Ti6Al4V substrate and PVA/HA/PAA/PDA hydrogel when the Ti6Al4V substrate treated with PDA or without PDA. (e) Representative curve of the peeling force per width of the hydrogel versus displacement. (f) Interfacial toughness of hydrogels bonded on Ti6Al4V measured by 90° peeling test. (g) XPS spectra and (h) EDS spectra of the Ti6Al4V after hydrogel was peeled. (i, j) SEM images of the Ti6Al4V surface after hydrogel was peeled.

standard 90° peel test. Figure 6(e) showed the force versus displacement curve of the hydrogel peeling from Ti6Al4V substrate. The combination of the Ti6Al4V substrate without PDA modification and the hydrogel belongs to mechanical interlocking (physical combination), the hydrogel can easily peel from the interface without significant deformation of the hydrogel, so that the stress required for the peeling of the hydrogel was small, and the corresponding interface toughness was only ~480 J/m^2. On the contrary, the combination of the PDA-modified Ti6Al4V substrate and the hydrogel belongs to the interaction of mechanical interlocking and chemical adhesion. The peeling of the hydrogel goes through

three stages. In the first stage, the hydrogel around the front of the interface crack was highly deformed as the peeling stress increased, and no separation between the hydrogel and the substrate. In the second stage, the drop in the peeling stress indicated that the interface cracks have begun to expand and the boundary edge of the hydrogel and the Ti6Al4V substrate has begun to separate. In the third stage, the peeling force reached a steady-state, and the crack spread along with the interface until it is completely peeled off [36, 42]. The measured interfacial toughness was ~3,900 J/m^2 (Fig. 6(f)), which is much higher than that of the tendon-bone, cartilage-bone interface [43, 44], and most hydrogel-substrate interfaces [16, 19, 35, 36, 45–48].

To further reveal the binding mechanism between the hydrogel and the PDA-LTi6Al4V substrate, the substrate was characterized by SEM, EDS, XPS after the hydrogel was peeled off. Figure 6(g) showed the characteristic peaks of Ca and P elements in the XPS spectrum of the substrate, indicating that there was residual nHA on the surface of the substrate after the hydrogel was peeled off. The EDS spectrums showed that there was hardly any Ti element in the middle area of the microporous array on the Ti6Al4V surface after the hydrogel was peeled, while the C, O, and N elements significantly increased (Figs. 6(d) and 6(h)). In summary, it is proved that the red area in Fig. 6(h) was covered with the residual hydrogel, which indicated the excellent binding between the hydrogel the Ti6Al4V substrate. On the other hand, the morphology of the microporous area was characterized after the hydrogel layer was peeled. It can be seen from Fig. 6(c) that there were micropores with an inner diameter of about 100 μm on the surface of the Ti6Al4V. However, there was residual hydrogel in the laser micropores on the Ti6Al4V surface after the hydrogel was peeled off, indicating that the hydrogel was embedded in the laser micropores, and the laser micropores play a role in mechanical interlocking (Fig. 6(i)). In addition, Fig. 6(j) showed that the residual hydrogel in the laser micropores adheres to the inner wall of the micropores in a filamentous shape, similar to the "foot silk" of mussels. It can be inferred that the PDA will adhere to the inner wall of the micropore when the Ti6Al4V substrate was modified with PDA. The adhesion effect of PDA makes the hydrogel tightly adhere to the substrate and the inner wall of the micropores, further enhancing the binding between the hydrogel and the substrate.

3.4 Tribological properties

In the various applications of soft-hard integrated materials, its practical application as an artificial joint requires excellent tribological properties. Therefore, the tribological properties of Ti6Al4V-hydrogel soft-hard integrated materials were studied through sliding friction, torsional friction, and swing friction experiments by simulating the motion form of the human body.

The sliding tribological properties of Ti6Al4V-hydrogel (PVA/HA/PAA/PDA) are better than Ti6Al4V-hydrogel (PVA/HA/PAA), which indicated that the addition of PDA can improve the tribological properties of the Ti6Al4V-hydrogel materials (Fig. 7(a)). On the one hand, the addition of PDA improves the compactness of the hydrogel network structure. The compressive strength of Ti6Al4V-hydrogel (PVA/HA/PAA/PDA) is significantly better than Ti6Al4V-hydrogel (PVA/HA/PAA) (Fig. 7). Therefore, the deformation of the PVA/HA/PAA/PDA hydrogel layer was smaller relatively under the same load, so that the frictional resistance generated by hydrogel deformation during sliding friction was reduced, which is manifested as a lower friction coefficient (Fig. 7(b)). Moreover, the introduction of PDA also can improve the surface roughness of the hydrogel, lowering the coefficient of friction.

We further studied the effects of load and sliding speed on tribological properties. Figure 7(c) showed the average friction coefficient of Ti6Al4V-hydrogel (PVA/HA/PAA/PDA) under the load of 20, 30, and 40 N, respectively. It can be seen that as the load increased, the friction coefficient increased. When the load is 20 and 40 N, the friction coefficient is 0.065 and 0.117, respectively. The increase of the load caused greater deformation of the hydrogel, which lead to the frictional resistance generated by the deformation of the hydrogel increased during the sliding process, so the friction coefficient became larger. Also, the greater load caused the lubricant to diffuse from the surface of the hydrogel, resulting in a higher friction coefficient. In different sliding speeds (5, 20, and 35 mm/s), the

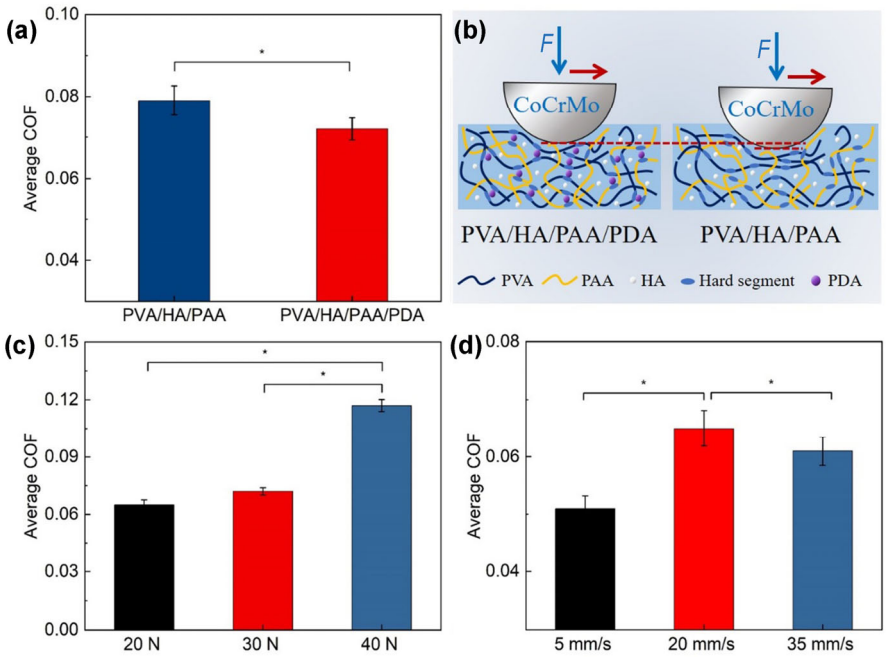

Fig. 7 (a) Average sliding friction coefficient of Ti6Al4V-PVA/HA/PAA hydrogel and Ti6Al4V-PVA/HA/PAA/PDA hydrogel. (b) Schematic diagram of sliding friction of Ti6Al4V-PVA/HA/PAA hydrogel and Ti6Al4V-PVA/HA/PAA/PDA hydrogel. Average friction coefficient of Ti6Al4V-PVA/HA/PAA/PDA Hydrogel under (c) different loads and (d) different sliding speeds.

friction coefficient first increased and then decreased, and its changing law conformed to the adsorption-repulsion model [49] (Fig. 7(d)). The sliding friction between CoCrMo and hydrogel was mainly affected by two factors: on the one hand, it originates from the elastic deformation force generated by the stretching of the polymer chain of the hydrogel. On the other hand, it comes from the lubrication of the hydration layer between the hydrogel and the ball, and its resistance was manifested by the viscous force of the hydration layer. The friction between the hydrogel and CoCrMo manifested as elastic friction at a lower sliding speed; On the contrary, it is mainly manifested as fluid lubrication when the sliding speed is higher.

The tribological dynamic characteristics of the torsional friction interface were exhibited by the friction torque–angular displacement (T–θ) curve [50]. As shown in Figs. 8(a)–8(c), the torque value gradually increased as the cycles of torsional friction increased, and the T–θ curve changed from a regular parallelogram to a narrower parallelogram-like shape, indicating that the motion state between the hydrogel and the CoCrMo interface has changed from a completely slip state to a stick–slip mixed state. The hydrogel layer of the Ti6Al4V-hydrogel materials is a viscoelastic material with high moist content. At the initial stage, the interface between the hydrogel and the CoCrMo ball was in a completely lubricated state, showing the liquid-phase loading and the lower sliding resistance. As the cycles increases, the fluid was extruded from the interface and the fluid load support decreased, resulting in the lubrication state of the friction interface change from full slip state into stick-slip state [51, 52]. Therefore, both the torque and the equivalent friction coefficient showed a rapid increase at the beginning of torsion, and it slowly increased until stable with the increase of the period.

In addition, the torque and the coefficient of friction were affected by the load. As the load increased, the friction torque increased (Figs. 8(a)–8(d)). As shown in Fig. 8(d), the torque at a load of 800 N (0.313 N/m) is much greater than that at a load of 400N (0.216 N/m). Conversely, the equivalent friction coefficient decreased as the load increased. the equivalent friction coefficient (0.0463) at a load of 800 N is much smaller than when the load is 400 N (0.0978).

The torsional friction performance of Ti6Al4V-hydrogel materials was also affected by the torsional angle. Figures 9(a)–9(d) showed the T–θ curves under different twisting angles, and the change law

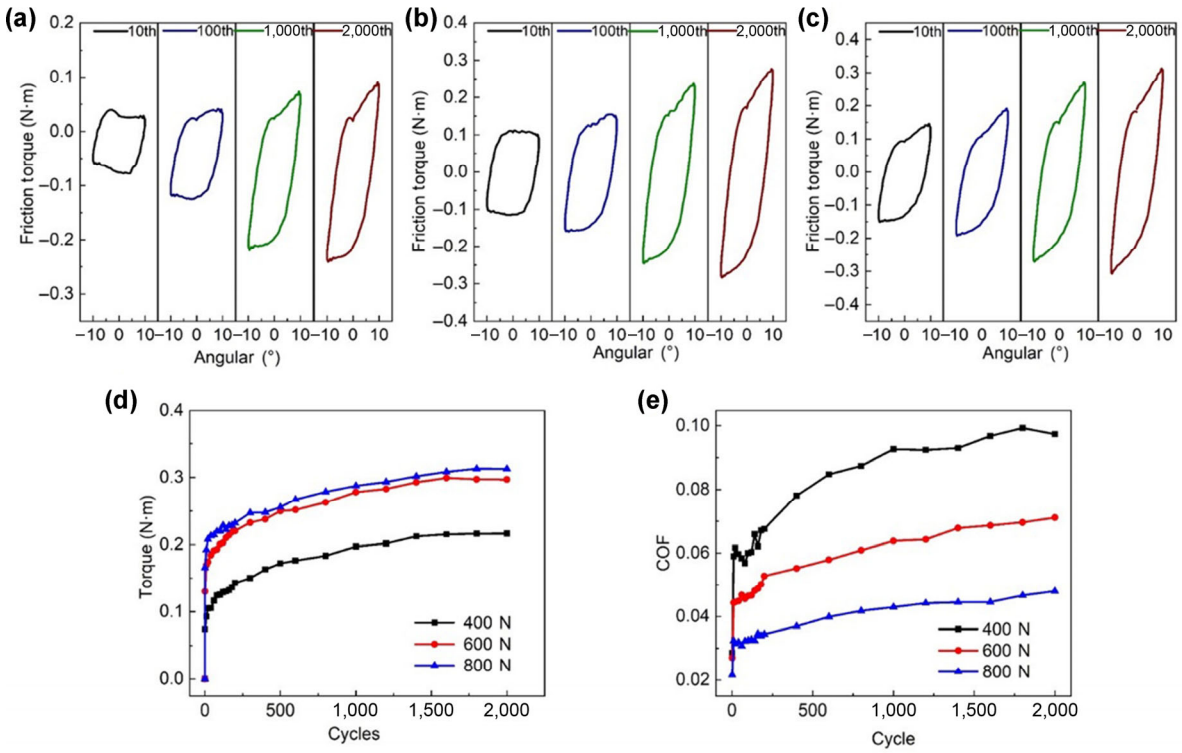

Fig. 8 Torsional tribological properties of Ti6Al4V-PVA/HA/PAA/PDA hydrogel soft-hard integrated material under different loads. Friction torque–angular displacement (T–θ) curve under (a) 400 N, (b) 600 N, and (c) 800 N. (d) Friction torque and (e) equivalent friction coefficient under different loads.

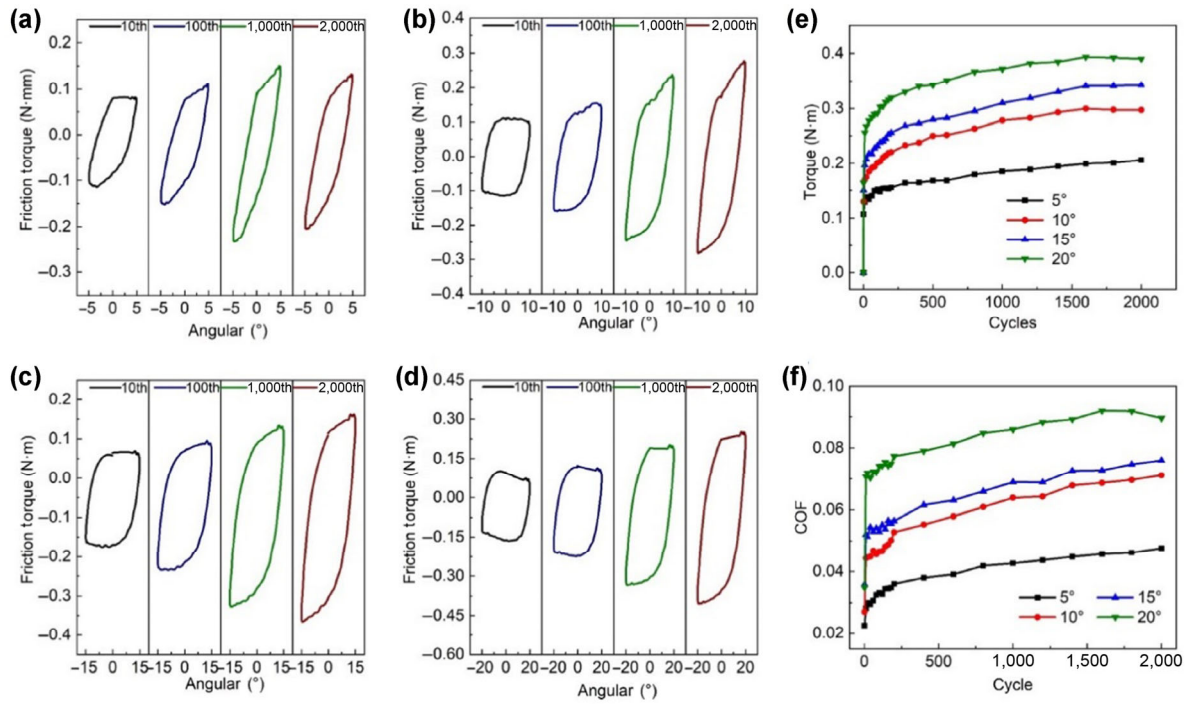

Fig. 9 Torsional tribological properties of Ti6Al4V-PVA/HA/PAA/PDA hydrogel soft-hard integrated material under different twisting angles. The friction torque–angular displacement (T–θ) curve under (a) 5°, (b) 10°, (c) 15°, and (d) 20°. (e) Friction torque and (f) equivalent friction coefficient under different twisting angles.

of the curves with the increase of the twisting friction cycle was consistent with that in Figs. 8(a)–8(c). Figures 9(e) and 9(f) showed the friction torque and equivalent friction coefficient under different torsional angles. The results showed that the friction torque and equivalent friction coefficient increased gradually with torsional angle, which results from the tangential force of the friction interface between the hydrogel and the CoCrMo ball increased with the increase of torsional angle. Moreover, with the increase of the torsional angle, the fluid flow velocity of hydrogel increase will lead to the decrease of lubrication, leading increase of friction torque and equivalent friction coefficient.

Similarly, the swing friction coefficient was affected by the load and swing angle (Fig. 10). As the load increased, the swing friction coefficient increased (Fig. 10(a)). On the one hand, the increase of load will increase the deformation of the hydrogel, and the contact area between the CoCrMo and the hydrogel will increase, resulting in the increase of resistance in the swing process. On the other hand, the greater load caused the lubricant to diffuse from the surface of the hydrogel, resulting in a higher friction coefficient. However, the friction coefficient can still be maintained at 0.096 under the high load of 200 N. Similarly, the swing friction coefficient increased as the swing angle increased (Fig. 10(c)). The fluid loss at the surface of the hydrogel accelerated with the increase of the swing angle, which weakened the liquid phase lubrication and fluid load support of the hydrogel layer, causing the increase of the friction force during the swing process. In addition, the swing angle has a greater influence on the coefficient of friction. When the swing angle is 20°, the friction coefficient (0.365) is 3 times larger than the swing angle of 5° (0.0836).

Figures 10(b) and 10(d) showed the reaction forces of Ti6Al4V-hydrogel materials in a swing cycle under different loads and swing angles, respectively. As the load increased and the swing angle increased, the reaction forces increased, which is the same as the results of the swing friction coefficient. The change curve of the frictional force in the swing direction in a cycle is similar to a sinusoidal curve. At the beginning of a cycle (0 s), the reaction force is 0 due to there no relative motion between the CoCrMo ball and hydrogel

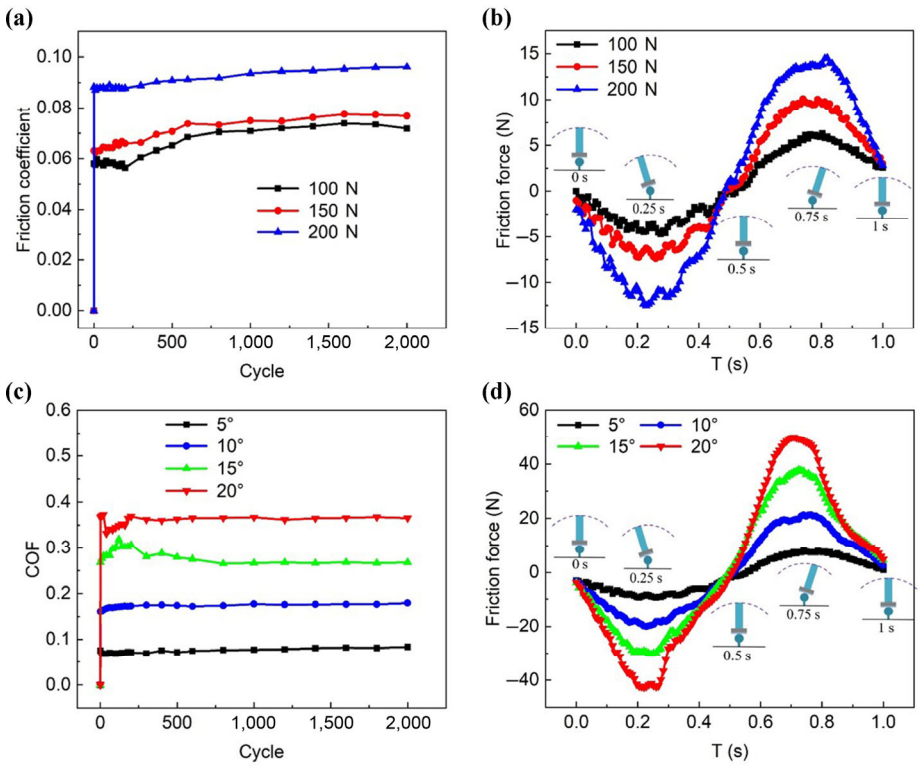

Fig. 10 Swing tribological properties of Ti6Al4V-PVA/HA/PAA/PDA hydrogel soft-hard integrated material. Swing friction coefficient under (a) different loads and (c) different swing angles. Reaction forces in friction direction under (b) different loads and (d) different swing angles.

layer in the frictional direction. Once the swing friction test begins, the reaction force increased rapidly in the negative direction until the swing angle reached the maximum (0.25 s). Subsequently, the swing friction gradually returned to the position of 0°, and the reaction force (negative) gradually decreased. When the CoCrMo ball returned to 0° (0.5 s), the reaction force in the frictional direction decreased to 0. The process mechanism of 0.5–1 s is the same as 0–0.5 s, and the reaction force direction is opposite.

Generally speaking, the friction force in the friction process is mainly derived from the shear force. According to the results of tribological properties, the maximum frictional force (shear force) of sliding friction, torsional friction and swinging friction is tens or tens of Newtons. However, according to the results of the interface toughness, the binding force between the hydrogel layer and the Ti6Al4V substrate is about 100 N, which is much larger than the frictional shear force. Therefore, the excellent binding performance between the hydrogel and the Ti6Al4V substrate can prevent the separation of the Ti6Al4V-hydrogel material during friction process. Overall, The Ti6Al4V-hydrogel materials possess ultra-high interfacial toughness and excellent tribological properties, which can be used as a candidate for artificial joints.

4 Conclusions

Inspired by the structure and function of natural articular cartilage, this work developed a soft-hard integrated material with an excellent tribological performance by laser printing, polydopamine (PDA) modification, and freezing-thawing, which simulated the natural cartilage-subchondral bone. The hydrogel lubricating layer was fixed on the surface of the titanium alloy by mechanical interlocking and chemical adhesion. The interface between the hydrogel and the Ti6Al4V substrate exhibited excellent binding performance that the normal bonding strength and interface toughness are as high as 52.7 MPa and 3,900 J/m^2, respectively, which are better than the tendon-bone interface, cartilage-bone interface, and most hydrogel-substrate interfaces. In addition, the results showed that the PDA can significantly enhance the interface binding performance to obtain a tough soft-hard (hydrogel-Ti6Al4V) interface. The function of PDA to design a strong soft-hard interface makes various research directions and applications possible in the future. Moreover, the Ti6Al4V-hydrogel exhibited excellent tribological performance, which was mainly attributed to the excellent lubricating performance of the hydrogel and the high mechanical properties of the Ti6Al4V. This simple method was expected to be used in the development of medical wear-resistant materials, and has broad prospects in the field of artificial joint implants.

Acknowledgements

This work was financially supported by Natural Science Foundation of Jiangsu Province (Grant No. BK20211243), National Natural Science Foundation of China (Grant Nos. 51705517, 51875563, 51875564), the Tribology Science Fund of State Key Laboratory of Tribology (Grant No. SKLTKF21B15) and the Open Fund of State Key Laboratory of Solid Lubrication, Lanzhou Institute of Chemical Physics (Grant No. LSL-2107).

References

[1] Forster H, Fisher J. The influence of loading time and lubricant on the friction of articular cartilage. *Proc Inst Mech En Part H-J Eng Med* **210**(2): 109–119 (1996)

[2] Macirowski T, Tepic S, Mann R W. Cartilage stresses in the human hip joint. *J Biomech Eng* **116**(1): 10–18 (1994)

[3] Devitt B M, Bell S W, Webster K E, Feller J A, Whitehead T S. Surgical treatments of cartilage defects of the knee: Systematic review of randomised controlled trials. *Knee* **24**(3): 508–517 (2017)

[4] Chuah Y J, Peck Y, Lau J E J, Heec H T, Wang D A. Hydrogel based cartilaginous tissue regeneration: recent insights and technologies. *Biomater Sci* **5**(4): 613–631 (2017)

[5] Rahaman M N, Yao A H, Bal B S, Garino J P, Ries M D. Ceramics for prosthetic hip and knee joint replacement. *J Am Ceram Soc* **90**(7): 1965–1988 (2007)

[6] Ingham E, Fisher J. Biological reactions to wear debris in total joint replacement. *Proc Inst Mech En Part H-J Eng Med* **214**(H1): 21–37 (2000)

[7] Chen K, Liu J L, Yang X H, Zhang D K. Preparation, optimization and property of PVA-HA/PAA composite hydrogel. *Mater Sci Eng C-Mater Biol Appl* **78**: 520–529 (2017)

[8] Long M, Rack H J. Titanium alloys in total joint replacement—A materials science perspective. *Biomaterials* **19**(18): 1621–1639 (1998)

[9] Standert V, Borcherding K, Bormann N, Schmidmaier G, Grunwald I, Wildemann B. Antibiotic-loaded amphora-shaped pores on a titanium implant surface enhance osteointegration and prevent infections. *Bioact Mater* **6**(8): 2331–2345 (2021)

[10] Palmquist A, Snis A, Emanuelsson L, Browne M, Thomsen P. Long-term biocompatibility and osseointegration of electron beam melted, free-form-fabricated solid and porous titanium alloy: Experimental studies in sheep. *J Biomater Appl* **27**(8): 1003–1016 (2013)

[11] Jinno T, Goldberg V M, Davy D, Stevenson S. Osseointegration of surface-blasted implants made of titanium alloy and cobalt-chromium alloy in a rabbit intramedullary model. *J Biomed Mater Res* **42**(1): 20–29 (1998)

[12] Park J W, Park K B, Suh J Y. Effects of calcium ion incorporation on bone healing of Ti6Al4V alloy implants in rabbit tibiae. *Biomaterials* **28**(22): 3306–3313 (2007)

[13] Sott A H, Rosson J W. The influence of biomaterial on patterns of failure after cemented total hip replacement. *Int Orthop* **26**(5): 287–290 (2002)

[14] Zhang C, Liu Z, Liu Y, Ren J, Cheng Q, Yang C, Cai L. Novel tribological stability of the superlubricity poly (vinylphosphonic acid) (PVPA) coatings on Ti6Al4V: Velocity and load independence. *Appl Surf Sci* **392**: 19–26 (2017)

[15] Wang K, Xiong D. Construction of lubricant composite coating on Ti6Al4V alloy using micro-arc oxidation and grafting hydrophilic polymer. *Mater Sci Eng C-Mater Biol Appl* **90**: 219–226 (2018)

[16] Zhao Z T, Gao W W, Bai H. A mineral layer as an effective binder to achieve strong bonding between a hydrogel and a solid titanium substrate. *J Mat Chem B* **6**(23): 3859–3864 (2018)

[17] Chen K, Chen G Y, Wei S, Yang X H, Zhang D K, Xu L M. Preparation and property of high strength and low friction PVA-HA/PAA composite hydrogel using annealing treatment. *Mater Sci Eng C-Mater Biol Appl* **91**: 579–588 (2018)

[18] Yang F C, Zhao J C, Koshut W J, Watt J, Riboh J C, Gall K, Wiley B J. A Synthetic hydrogel composite with the mechanical behavior and durability of cartilage. *Adv Funct Mater* **30**(36): 202003451 (2020)

[19] Cui L L, Chen J Y, Yan C Q, Xiong D S. Articular Cartilage Inspired the Construction of LTi-DA-PVA Composite Structure with Excellent Surface Wettability and Low Friction Performance. *Tribol Lett* **69**(2): 41 (2021)

[20] Zhou H J, Xiong D S, Tong W, Shi Z B, Xiong X Y. Lubrication behaviors of PVA-casted LSPEEK hydrogels in artificial cartilage repair. *J Appl Polym Sci* **136**(37): 47944 (2019)

[21] Baker M I, Walsh S P, Schwartz Z, Boyan B D. A review of polyvinyl alcohol and its uses in cartilage and orthopedic applications. *J Biomed Mater Res Part B* **100B**(5): 1451–1457 (2012)

[22] Zhang Y S, Khademhosseini A. Advances in engineering hydrogels. *Science* **356**(6337): eaaf3627 (2017)

[23] Gu Z P, Huang K Q, Luo Y, Zhang L B, Kuang T R, Chen Z, Liao G C. Double network hydrogel for tissue engineering. *Wiley Interdiscip Rev-Nanomed Nanobiotechnol* **10**(6): e1520 (2018)

[24] Zhao Z G, Fang R C, Rong Q F, Liu M J. Bioinspired nanocomposite hydrogels with highly ordered structures. *Adv Mater* **29**(45): 1703045 (2017)

[25] Vaz C M, Reis R L, Cunha A M. Use of coupling agents to enhance the interfacial interactions in starch-EVOH/ hydroxylapatite composites. *Biomaterials* **23**(2): 629–635 (2002)

[26] Arts J J C, Verdonschot N, Schreurs B W, Buma P. The use of a bioresorbable nano-crystalline hydroxyapatite paste in acetabular bone impaction grafting. *Biomaterials* **27**(7): 1110–1118 (2006)

[27] Zhang D K, Duan J J, Wang D G, Ge S R. Effect of preparation methods on mechanical properties of PVA/HA composite hydrogel. *J Bionic Eng* **7**(3): 235–243 (2010)

[28] Li W X, Wang D, Yang W, Song Y. Compressive mechanical properties and microstructure of PVA-HA hydrogels for cartilage repair. *RSC Adv* **6**(24): 20166–20172 (2016)

[29] Cheng Y Z, Hu Y C, Xu M J, Qin M, Lan W W, Huang D, Wei Y, Chen W Y. High strength polyvinyl alcohol/polyacrylic acid (PVA/PAA) hydrogel fabricated by Cold-Drawn method for cartilage tissue substitutes. *J Biomater Sci - Polym Ed* **31**(14): 1836–1851 (2020)

[30] Faturechi R, Karimi A, Hashemi A, Yousefi H, Navidbakhsh M. Influence of poly(acrylic acid) on the mechanical properties of composite hydrogels. *Adv Polym Technol* **34**(2): 21487 (2015)

[31] Gulyuz U, Okay O. Self-healing poly(acrylic acid) hydrogels with shape memory behavior of high mechanical strength. *Macromolecules* **47**(19): 6889–6899 (2014)

[32] Chen K, Zhang D K, Cui X T, Wang Q L. Preparation of ultrahigh-molecular-weight polyethylene grafted with polyvinyl alcohol hydrogel as an artificial joint. *RSC Adv* **5**(31): 24215–24223 (2015)

[33] Zhao Z T, Gao W W, Bai H. A mineral layer as an effective binder to achieve strong bonding between a hydrogel and a solid titanium substrate. *J Mat Chem B* **6**(23): 3859–3864 (2018)

[34] Cheng H, Yue K, Kazemzadeh-Narbat M, Liu Y H, Khalilpour A, Li B Y, Zhang Y S, Annabi N, Khademhosseini A. Mussel-inspired multifunctional hydrogel coating for prevention of infections and enhanced osteogenesis. *ACS Appl Mater Interface* **9**(13): 11428–11439 (2017)

[35] Kurokawa T, Furukawa H, Wang W, Tanaka Y, Gong J P. Formation of a strong hydrogel-porous solid interface via the double-network principle. *Acta Biomater* **6**(4): 1353–1359 (2010)

[36] Yuk H, Zhang T, Lin S T, Parada G A, Zhao X H. Tough bonding of hydrogels to diverse non-porous surfaces. *Nat Mater* **15**(2): 190–196 (2016)

[37] Han L, Lu X, Liu K Z, Wang K F, Fang L M, Weng L T, Zhang H P, Tang Y H, Ren F Z, Zhao C C, Sun G X, Liang R, Li Z J. Mussel-inspired adhesive and tough hydrogel based on nanoclay confined dopamine polymerization. *ACS Nano* **11**(3): 2561–2574 (2017)

[38] Jing X, Mi H Y, Lin Y J, Enriquez E, Peng X F, Turng L S. Highly stretchable and biocompatible strain sensors based on mussel-inspired super-adhesive self-healing hydrogels for human motion monitoring. *Acs Appl Mater Interfaces* **10**(24): 20897–20909 (2018)

[39] Su T, Zhang M Y, Zeng Q K, Pan W H, Huang Y J, Qian Y N, Dong W, Qi X L, Shen J L. Mussel-inspired agarose hydrogel scaffolds for skin tissue engineering. *Bioact Mater* **6**(3): 579–588 (2021)

[40] Tang Z W, Miao Y N, Zhao J, Xiao H, Zhang M, Liu K, Zhang X Y, Huang L L, Chen L H, Wu H. Mussel-inspired biocompatible polydopamine/carboxymethyl cellulose/polyacrylic acid adhesive hydrogels with UV-shielding capacity. *Cellulose* **28**(3): 1527–1540 (2021)

[41] Chen K, Liu S Y, Wu X F, Wang F Y, Chen G Y, Yang X H, Xu L M, Qi J W, Luo Y, Zhang D K. Mussel-inspired construction of Ti6Al4V-hydrogel artificial cartilage material with high strength and low friction. *Mater Lett* **265**: 127421 (2020)

[42] Biggins J S, Saintyves B, Wei Z Y, Bouchaud E, Mahadevan L. Digital instability of a confined elastic meniscus. *Proc Natl Acad Sci U S A* **110**(31): 12545–12548 (2013)

[43] Bobyn J D, Wilson G J, MacGregor D C, Pilliar R M, Weatherly G C. Effect of pore size on the peel strength of attachment of fibrous tissue to porous-surfaced implants. *J Biomed Mater Res* **16**(5): 571–584 (1982)

[44] Moretti M, Wendt D, Schaefer D, Jakob M, Hunziker E B, Heberer M, Martin I. Structural characterization and reliable biomechanical assessment of integrative cartilage repair. *J Biomech* **38**(9): 1846–1854 (2005)

[45] Yuk H, Zhang T, Parada G A, Liu X Y, Zhao X H. Skin-inspired hydrogel-elastomer hybrids with robust interfaces and functional microstructures. *Nat Commun* **7**: 12028 (2016)

[46] Zhang Y X, Ren B P, Xie S W, Cai Y Q, Wang T, Feng Z Q, Tang J X, Chen Q, Xu J X, Xu L J, Zheng J. Multiple physical cross-linker strategy to achieve mechanically tough and reversible properties of double-network hydrogels in bulk and on surfaces. *Acs Appl Polym Mater* **1**(4): 701–713 (2019)

[47] Xu J Y, Gao G H, Duan L J, Sun G X. Protein and hydrophobic association-regulated hydrogels with adhesive adjustability in different materials. *Adv Mater Interfaces* **7**(1): 1901541 (2020)

[48] Zhang Y K, Xue J J, Li D P, Li H Y, Huang Z H, Huang Y W, Gong C J, Long S J, Li X F. Tough hydrogels with tunable soft and wet interfacial adhesion. *Polym Test* **93**: 106976 (2021)

[49] Gong J P. Friction and lubrication of hydrogels - its richness and complexity. *Soft Matter* **2**(7): 544–552 (2006)

[50] Chen K, Zhang D K, Yang X H, Cui X T, Zhang X, Wang Q L. Research on torsional friction behavior and fluid load support of PVA/HA composite hydrogel. *J Mech Behav Biomed Mater* **62**: 182–194 (2016)

[51] Cai Z B, Gao S S, Gan X Q, Yu H Y, Zhu M H. Torsional fretting wear behaviour of nature articular cartilage in vitro. *Int J Surf Sci Eng* **5**(5–6): 348–368 (2011)

[52] Gan X Q, Cai Z B, Qiao M T, Gao S S, Zhu M H, Yu H Y. Fretting wear behaviors of mandibular condylar cartilage of nature temporomandibular joint in vitro. *Tribol Int* **63**: 204–212 (2013)

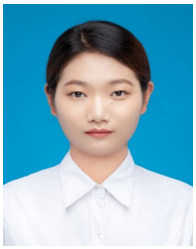

Qin CHEN. She will receive her M.D. degree at China University of Mining and Technology in 2022. Her current research interests mainly focus on the bionic design of functional materials and tribology of soft materials.

Xinyue ZHANG. She is a Ph.D. candidate at China University of Mining and Technology. She is a joint Ph.D. student at the University of British Columbia (UBC) from 2021 to 2022. She has published 6 papers. Her current research interests cover the bionic design of functional materials, tribology of soft materials, and bio-tribology of artificial joints.

Kai CHEN. He received his Ph.D. degree from China University of Mining and Technology in 2015. He is currently an associate professor at China University of Mining and Technology. He has published over 50 papers and applied for 10 patents. His current research interests cover the bionic design of functional materials, tribology of soft materials, bio-tribology of artificial joints, and wear-resistant materials.

Dekun ZHANG. He received his Ph.D. degree from China University of Mining and Technology in 2003. He is a professor at China University of Mining and Technology since 2008. His current research interests cover fretting, friction reliability of mining machinery, bio-tribology of artificial joints, bionic design of functional materials, and wear-resistant materials etc. He has published 2 monographs, more than 180 papers, of which over 100 publications are included in SCI, and he has also obtained more than 30 patents for invention. His main academic part-time jobs include the deputy chairman of the Tribological Branch of the Chinese Mechanical Engineering Society, the chairman of the Tribological Branch of the Jiangsu Mechanical Engineering Society, etc.